Int. J. Electrochem. Sci., 9 **(2014)** 195 - 205

International Journal of
ELECTROCHEMICAL
SCIENCE
www.electrochemsci.org

Effects of the Mass Balance Ratio and the Cut-off Voltage on the Performance of a Graphite (KS-6)/TiO_2 (Anatase) Energy Storing System

Nanda Gunawardhana[1,2,*], *Gum-Jae Park*[2], *Nikolay Dimov*[2] , *Hongyu Wang*[2], *Manickam Sasidharan*[3], *Arjun Kumar Thapa*[2], *Hiroyoshi Nakamura*[3] *and Masaki Yoshio*[2,*]

[1] International Research Centre, University of Peradeniya, Peradeniya, Sri Lanka.
[2] Advanced Research Center, Saga University, 1341 Yoga-machi, Saga 840-0047, Japan.
[3] Department of Chemistry and Applied Chemistry, Saga University, 1 Honjo, Saga 840-8502, Japan.
[*]E-mail: nandagunawardhana@pdn.ac.lk; yoshio@cc.saga-u.ac.jp

Received: 4 September 2013 / *Accepted:* 12 October 2013 / *Published:* 15 November 2013

The performance of KS-6/TiO_2 full cell has been studied at different cut-off voltages, charge/discharge rates and cathode to anode mass ratios. The charge/discharge mechanism of the full cell is elucidated by e*x-situ* XRD data and analyzing the voltage profiles of each electrode by means of 4-electrode cell. Capacity retention of the cell between the 3rd and 50th cycles is 95.5 % though the ceiling potential of KS-6 exceeds 5.1 V vs. Li/Li^+. Under such conditions this device delivers 100 $Wh.kg^{-1}$ based on the total weight of the cathode and anode materials. Thus the energy density of this device is higher than AC/TiO_2 type capacitors due to the higher working voltage and capacity of the KS-6 cathode. The KS-6:TiO_2 weight ratio and charging potential have a crucial influence on the overall performance of this device. The KS-6/TiO_2 weight ratio could be increased up to 2 without a significant capacity fade of the cell in the voltage window 1.5-3.5 V. These results demonstrate that the electrolyte could be used as the sole source of Li^+ allowing development of novel type of energy storage devices without lithium rich cathodes as the lithium source.

Keywords: Safety of Batteries, Titanium Oxide Anode, Graphite Cathode, Cathode to Anode Mass Ratio, Cycle Performance.

1. INTRODUCTION

Electrical energy storage is very important for many applications varying from small scale portable devices to electric and hybrid electric vehicles. To fulfill this demand, the rechargeable energy storage devices, such as lithium ion batteries (LIB) and electric double layer capacitors (EDLC) are

being widely used [1-6]. Recently, the capacitors have attracted various research groups because of their potential application as energy storage devices mainly due to high power density. However conventional EDLC having activated carbon electrodes show low energy density due to its low operating voltage, thus prevailing most of the commonly used applications. To enhance the energy density of traditional EDLCs, asymmetrical super capacitors were developed. In such a capacitor the activated carbon negative electrode was replaced by an electrode made of a lithium ion secondary battery [7-10]. Using this strategy the energy density of the asymmetric capacitor could be enhanced by increasing the voltage window and/or specific capacitance of the anode. In such conditions, the hybrid capacitor could only be operated in the limited potential window. To enlarge the potential window of positive electrode, we introduced graphite as a cathode in the organic electrolyte medium [11, 12]. This enables us to operate graphite as a cathode over 5.0 vs. Li/Li^+ without any safety issues. The energy density of such capacitors is expected to be higher compared to that of conventional EDLCs. In this approach the charge storage mechanism at the cathode consists of adsorption and intercalation of anions into the graphite layers.

Recently, we have developed a new electrochemical power source in which metal oxides and graphite are employed as the anode and the cathode, respectively [13-15]. This kind of electrochemical devices are inherently safer than lithium ion batteries and possess higher energy density than EDLC. In this regard we have tested some metal oxides so far. In our previous work, we have demonstrated KS-6/ TiO_2 as a novel energy storage system in which we described the basic concepts related to the energy storing system. Herein, we describe in detail, the features of a novel energy storage system composed of graphite (KS-6) cathode and TiO_2 (anatase) anode. The performance of this energy storage system was tested under different conditions. The mass balance of cathode to anode was carried out to optimize the performance of the full cell. After selecting the best cut-off voltage, the rate performance of the cells was studied. To understand the overall reaction mechanism, the voltage profiles were obtained by 4-electrode cell which was recording simultaneously the potential profiles of the half-cells Li/TiO_2 and Li/graphite. E*x-situ* XRD data were collected at fully charged and discharged states to get more insight of the structural changes of the KS-6 cathode and TiO_2 anode and thereby elucidating the absorption/intercalation mechanism of the full cell.

2. EXPERIMENTAL

Artificial graphite (KS-6, Timcal. Co. Ltd., Switzerland) was used as a cathode material and commercial TiO_2 (anatase TiO_2 from Ishihara Sangyo Co., Ltd., Japan) was used as an anode material. The electrodes were first dried at 120 ^oC then punched out into disks having 2 cm^2 cross sectional area. The electrochemical characterizations were performed using CR2032 coin-type cells. The electrodes were pressed under 300 kg cm^{-2} and vacuum dried at 160 ^oC for 4 h. The positive and negative electrodes were separated by two glass fiber filters and the amount of the electrolyte was ca. 0.5 mL. The electrolyte was 1.0 M $LiPF_6$ (Ethylene Carbonate/Dimethyl Carbonate (EC/DMC) =1/2 (v/v)) supplied by Ube Chemicals Co., Ltd., Japan. Mass loading of electrodes was 4-6 mg/cm^2. The cycle life test was carried out at a current density of 100 $mA.g^{-1}$. Powder X-ray diffraction (XRD, MINIFlex

Ⅱ, Rigaku, Japan) using CuKα radiation was employed to identify the intercalation of the PF_6^- anions and structural changes in positive and negative electrodes under various stages of charge. In such a test the coin cells were disassembled at a desired state of charge and both graphite and TiO_2 electrodes were recovered in an argon filled glove box. After being washed with DMC, the electrodes were sealed in polyvinyl bags to prevent any reaction with air and their XRD patterns were immediately recorded. Other experimental details and instrumentation methods are described elsewhere [11,12, 16-17].

3. RESULTS AND DISCUSSION

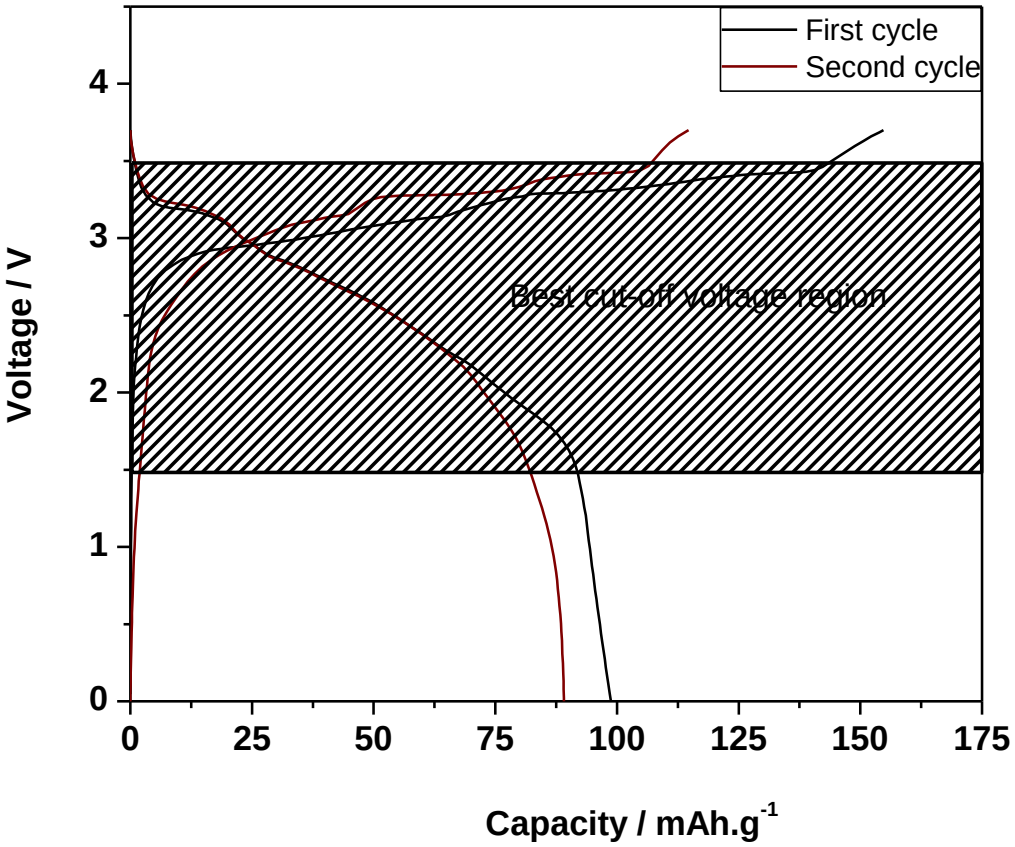

Figure 1. The initial charge/discharge curves of cell contain graphite (KS-6) cathode and TiO_2 (Anatase) in 1.0 M $LiPF_6$-EC/DMC(1:2) solution in the voltage region of 0.0-3.7 V. The charge/discharge current density is 100 mAg^{-1} and the mass ratio of the positive to negative electrode is one.

Figure 1 shows the first and second charge/discharge curves of the KS-6/TiO_2 energy storage system using 1.0 M $LiPF_6$ (EC/DMC=1/2 (v/v)) under a constant current of 1.0 mA in different voltage windows. The primary cut-off voltages were preset in the ranges of 0-3.7 V, 1.5-3.7 V, 0.0-3.5 and 1.5-3.5 V. In the voltage region of 0.0-3.7 the KS-6/TiO_2 cell delivered the initial charge capacity of

155 mAh.g^{-1} and the first discharge capacity was 99 mAhg^{-1}. From these results it can clearly be seen that the first cycles have significantly higher irreversible capacity. The coulombic efficiency of the first cycle is 63.9 %. The low coulombic efficiency in the first cycles could be attributed to two main factors: The irreversible capacity associated with TiO_2 anode and its electrolyte decomposition and the irreversible capacity associated with anion intercalation into the graphite and its partial exfoliation. We believe that the later process contributes more to the total irreversible capacity of TiO_2/KS-6 full cell. The voltage profile recorded by 4 the electrode cells revealed that the 3.7 V upper cut-off voltage of the TiO_2/KS-6 full cell corresponds to 5.35 V at the cathode vs. Li/Li$^+$. To avoid that we then decreased the upper cut-off voltage down to 3.5 V of the full cell. The charge capacities of the second cycle in the ranges of 0.0-3.7 and 0.0-3.5 were 114 and 107 mAh.g^{-1} while the discharge capacities in the same range were 91 and 75 mAh.g^{-1} respectively.

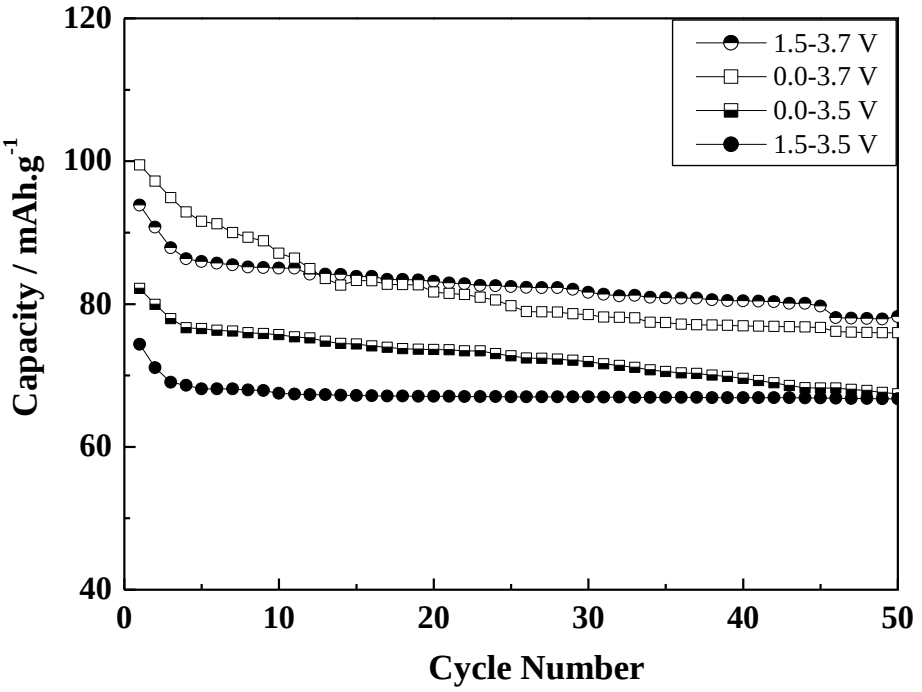

Figure 2. Cycleability of KS-6/TiO_2 cell with different cut-off voltages. The charge/discharge current density is 100 mAg^{-1} and the mass ratio of the positive to negative electrode is one.

Figure 2 shows the variation of discharge capacities of KS-6/TiO_2 system with various cut-off voltage windows. Although it deliver 99 mAh.g^{-1} during the first discharge, the capacity retention between 3rd and 50th cycle in the voltage region of 0.0-3.7 is 75.9 %. This indicates that the full depth of charge/discharge of the KS-6/TiO_2 cell may lead to significant capacity fading as the number of cycles increases. To improve the cyclability, an attempt was made to lower the upper cut-off voltage down to 3.5 V. Even though this causes a slight decrease in discharge capacity, as shown in Figure 2, the capacity retention in the voltage region 0.0-3.5 is better than that of 0.0-3.7 V and was found to be 86.3 % between the 3rd and 50th cycles. It is seen from voltage profiles, that increasing the lower cut-

off voltage from 0.0 to 1.0 V does not cause a significant decrease in the energy density of KS-6/TiO_2 system because the discharge curve between 1.5 and 0.0 V is almost vertical. Therefore we then have adjusted the bottom potential of the full cell. Increasing the lower cut-off voltage from 0.0 to 1.5 V showed a capacity of retention of 95.5% between the 3rd and 50th cycle. Therefore the best cut-off voltage window of the TiO_2/KS-6 energy storage device is 1.5-3.5 V which shown as a shaded rectangle in Figure 1.

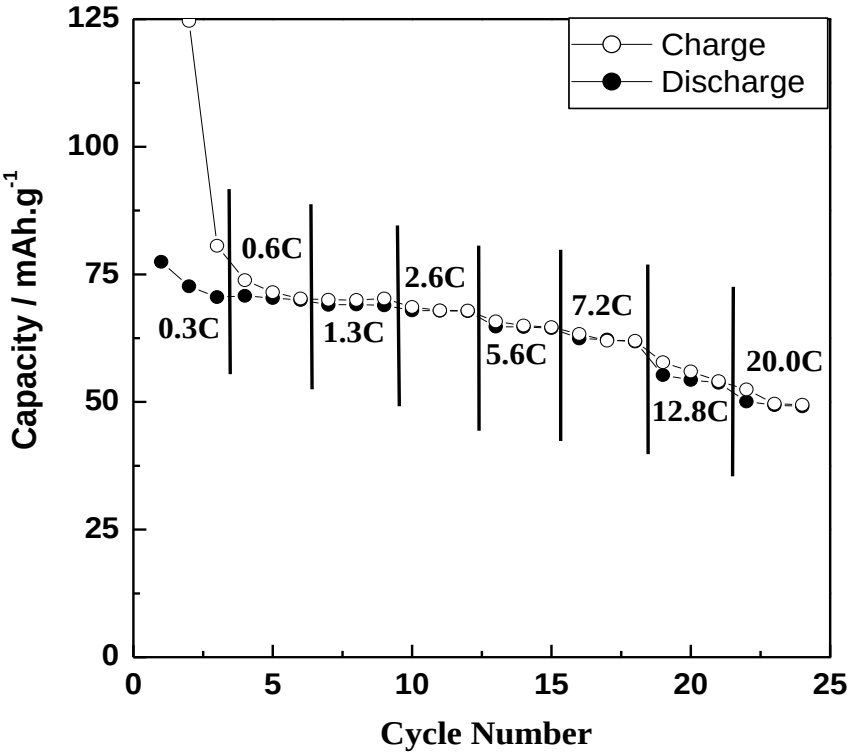

Figure 3. The rate performance of KS-6/TiO_2 capacitor in the voltage range of 1.5-3.5 V. The charge discharge current density at 1 C rate is ca. 100mAg^{-1}. The mass ratio of the positive to negative electrode is one.

Figure 3 exhibits the rate capabilities of KS-6/TiO_2 with a mass ratio of 1:1 in the voltage range of 1.5-3.5 V. At a 0.3 C rate, the discharge capacity of the cell is 78 mAh.g^{-1}. Since the charge/discharge curves are not flat, the average voltage, energy and power densities of this device were calculated by integrating the area under the capacity/voltage profile. Therefore, the calculated average voltage in the range of 1.5-3.5 of this cell is about 2.7 V. According to the total weight of active materials, KS-6/TiO_2 cell delivers 100 Wh Kg^{-1} as energy density in the voltage region of 1.5-3.5 V. As shown in Figure 3, when the charge/discharge rate increases, the specific capacities decrease gradually. At 20 C rate the discharge capacity of the cell drops down to 50 mAh.g^{-1}. Unlike traditional EDLC capacitors, at high charge/discharge rates the performance of the full cell of KS-6/TiO_2 gradually fades due to relatively slow kinetics of intercalation of ions into their respective electrodes

than that of the adsorption/desorption processes in the capacitors. This effect could be mainly attributed to the anion intercalation process of the cathode. However, even at 20 C rate the energy and power densities of this device are higher than that of Megalo-capacitance capacitors and AC/TiO_2 type hybrid capacitors [17-20]. This may be due to the fact that the simultaneous intercalation of Li^+ and PF_6^- ions to the anode and cathode. We believe that some kind of "synergistic" effect results in a good rate capability of this cell. Hence during intercalation/de-intercalation processes, ions might show higher kinetics in the full cell to maintain the charge balance of the solution. In addition, the higher charging voltage and larger discharge capacity of the working electrodes of the KS-6/TiO_2 full cell also causes the higher energy and power density of this device.

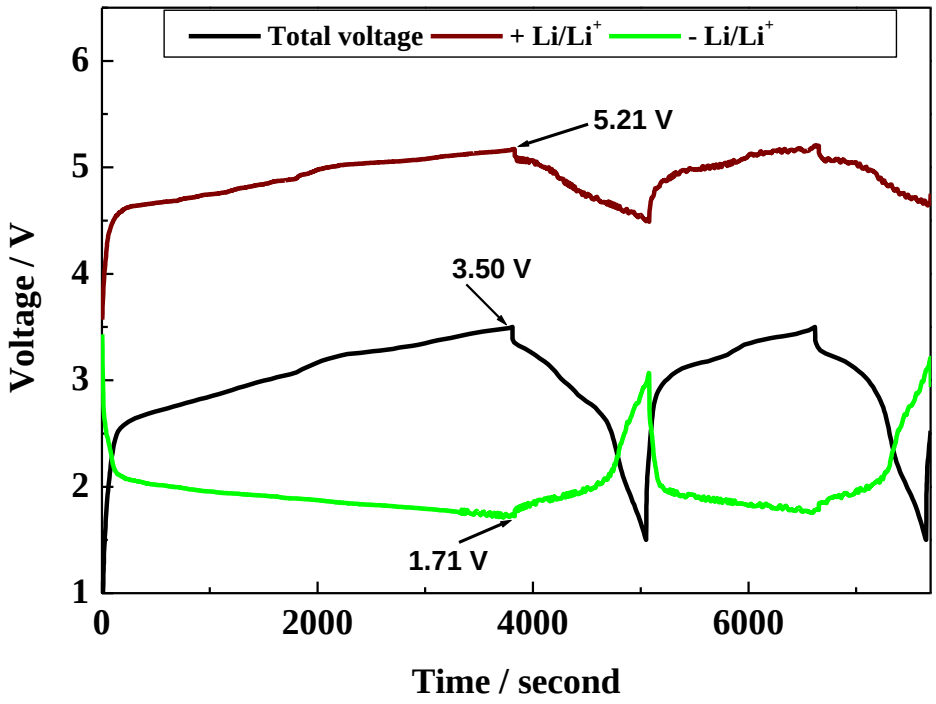

Figure 4. Potential profiles of KS-6/TiO_2 cell during the galvanostatic charge/discharge process in the voltage region 0.0-3.5 V. The positive and negative electrodes have the 10 mg of active material. The charge /discharge current density is 100 mAg^{-1} and the mass ratio of positive to negative electrode is one.

Figure 4 shows the potential profiles of the KS-6 positive and TiO_2 negative electrodes with respect to two Li metal reference electrodes in 1.0 M $LiPF_6$ (EC/DMC = 1/2 (v/v)) solution. During the first charging process, this device shows an initial sudden voltage increase up to 2.6 V but the capacity at this stage is small as the amount of the anions/cations adsorbed over the surfaces of KS-6 and TiO_2 are not appreciable. The BET surface area of bulk TiO_2 anode and KS-6 cathode are 8 and 18 m^2g^{-1}, respectively. This indicates that capacitive behaviors of the electrodes are negligible compared to that of Faradaic intercalation processes of the electrodes. This is mainly due to the lower surface area of

graphite and TiO_2 compared with that of activated carbon (1500-3500 m^2g^{-1}) which is commonly use in EDLCs. In the initial adsorption process, the potential of TiO_2 negative electrode drops down to 2.2 V vs. Li/Li^+. On the other hand, the potential of KS-6 cathode rises up to 4.7 V vs. Li/Li^+. When the charging voltage increases more than 2.6 V in the full cell, the Li^+ cation and PF_6^- anions start to intercalate to TiO_2 and KS-6, respectively. This indicates that the energy storage process in this cell is transferred from electric double layer electrostatic absorption to Faradaic energy storage. During the charging process of full cell up to 3.5 V, the potential of TiO_2 anode gradually drops down to 1.7 V vs. Li/Li^+ while the KS-6 electrode increases up to 5.2 V vs. Li/Li^+. These two intercalation processes cause a bent shape charging voltage profile of the full cell. As the voltage plateau of TiO_2 is not very sharp, the shape of the charging voltage curves is similar to that of KS-6. During the discharge process, the potential of TiO_2 gradually increases from 1.7 to 3.0 V vs. Li/Li^+, while the potential of KS-6 suddenly drops from 5.4 to 5.2 V vs. Li/Li^+, and then gradually decreases down to 4.5 V. These two processes maintain the voltage of this device between 1.5-3.5 V. Moreover, the first discharge time is significantly shorter than charging time. This is because of the electrolyte decomposition during the first charging process. However, the charge/discharge times of the second cycle do not show significant difference.

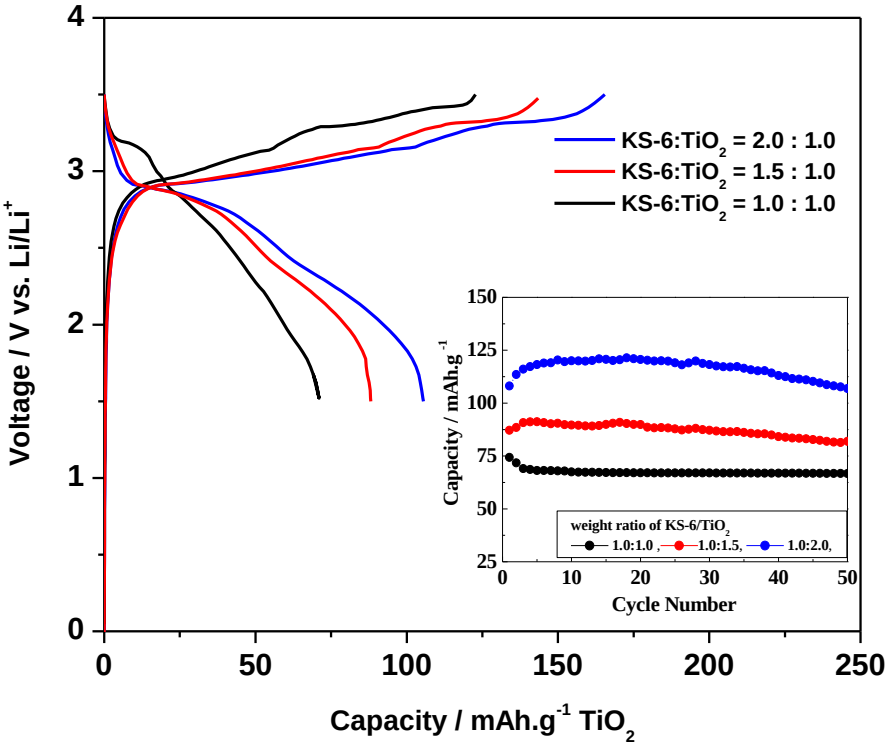

Figure 5. The effects of mass balance of KS-6:TiO_2 for the capacity and cycleability of cell in the voltage region 0.0-3.5 V. The charge /discharge current density is 100 mAg^{-1} and the mass ratio of positive to negative electrode is one.

In our previous communication we have used the same amount of active materials for cathode and anode. However, our preliminary results showed that the discharge and charge capacities of the

TiO_2/Li half-cell are 208 and 175 mAh.g^{-1} respectively in the voltage region of 1.0-3.0 V. In addition, the 4-electrode experiments revealed that the full discharge depth of TiO_2 was not attained because the capacity of the cell is limited on the positive electrode of the KS-6/TiO_2 full cell. Therefore, complete lithium insertion/extraction from the TiO_2 is not possible during the charge/discharge process of full cell. To extract the maximum capacity from TiO_2 anode, thereby enhancing the power and energy of this device, we then investigated the influence of the weight ratio of TiO_2 and KS-6 electrodes in the voltage region of 1.5-3.5 V. The figure 5 shows the charge/discharge profiles of the KS-6/TiO_2 cell with different mass ratios. When the mass ratio of KS-6/TiO_2 is 2 the initial charge capacity of the cell is 166 mAh.g^{-1}. However, this value decrease to 144 and 122 mAh.g^{-1} while decreasing the weight ration of KS-6/TiO_2 from 1.5 and then to 1.0 respectively. The shape of the charging curves does not change significantly. In the same voltage region, the discharge capacities under the mass ratios of KS-6/TiO_2 for 2, 1.5 and 1.0 are 105, 88 and 71 mAh.g^{-1}, respectively. The cycling behavior of the full cells with different KS-6 to TiO_2 mass ratios are shown in figure 5 (Inset). The capacity retention of the cell gradually decreases with increasing the weight ratio of KS-6/TiO_2. When the KS-6/TiO_2 ratio is 2, the first discharge capacity of the full cell is 107.73 mAh.g^{-1} but the capacity retention from the 5th to the 100th cycle becomes 75.8 %. By decreasing the weight ratio of KS-6/TiO_2 to 1.5, capacity retention of the full cell between the 5th and the 100th cycle increased up to 85.7 %. When we further decrease the mass ratio of KS-6/TiO_2 down to 1, the capacity retention of the cell between the 5th and the 100th cycles increased up to 96.3%. These experiments clearly suggest that at higher KS-6/TiO_2 weight ratios, the higher capacity possibly originated from the anode, but it reduces the cycling performance of the full cell. At this juncture, we are optimizing the cut-off voltages of the full cell with respect to each mass ratio to optimize the tradeoff between energy density and cyclability of this new energy storage device. By adjusting the cut-off voltages, we believe that the performance of the cell could be further improved because energy density, swing voltage, and specific capacitance are all functions of the electrode mass ratio and ionic concentration of the electrolyte.

We then employed 4-electrode cell experiments to gain further insight into the relative voltage changes of the KS-6/TiO_2 cell with respect to different mass ratios. Using this method we measured the ceiling- and bottom-voltages of KS-6/TiO_2 cell while increasing the weight ratio of cathode to anode from 1 to 2. The ceiling voltages of KS-6 electrode were decreased from 5.17 to 5.09 V by increasing the weight ratio of KS-6/TiO_2 system. On the other hand, the bottom voltages of TiO_2 anodes decreased simultaneously from 1.71 to 1.59 V maintaining the overall charging potential at 3.5 V. This experiment confirms that achieving good cyclability is possible only after precise adjustment of the cut-off voltages of both the cathode and anode. Even though high graphite/TiO_2 weight ratios cause the graphite positive electrode to be less burdened with low voltage load, this leads to relatively high capacity fading of the TiO_2 negative electrode. As we observed in the cycle test, increasing the weight ratio of the cathode to the anode may lead to some deterioration of the capacity with prolonged cycling. Recently we synthesized new titania nano spheres which shows higher capacity and cycle life under the full charge/discharge state [21]. We believe that this type of anode may give good cyclability at high cathode to anode weight ratios.

In order to investigate the reaction mechanism and structural changes of the cathode and anode, *ex-situ* XRD experiments were conducted.

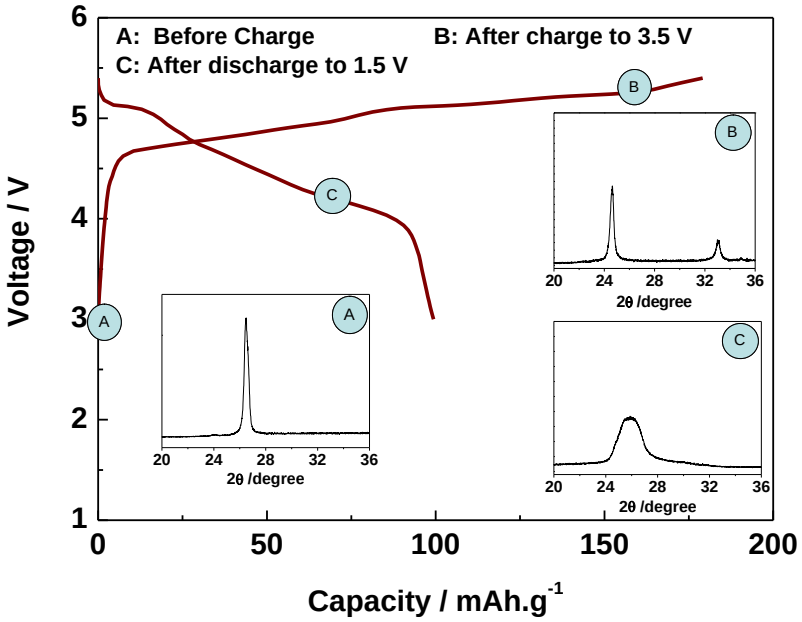

Figure 6. *Ex-situ* XRD patterns of the KS-6 electrode, after the first charge and discharge processes in the voltage region 0.0-3.5 V. The charge/discharge current density is 100 mAg^{-1} and the mass ratio of the positive to negative electrode is one.

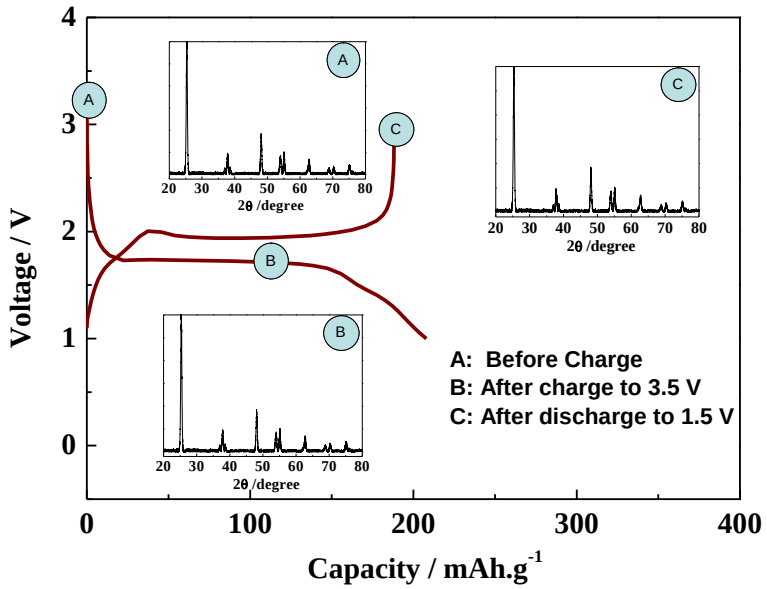

Figure 7. *Ex-situ* XRD patterns of the TiO_2 electrode, after the first charge and discharge processes in the voltage region 0.0-3.5 V. The charge/discharge current density is 100 mAg^{-1} the mass ratio of the positive to negative electrode is one.

Figures 6 and 7 show *ex-situ* XRD diffractions of the KS-6 and TiO_2 electrodes in the KS-6/TiO_2 energy storage system, before and after the first charge (3.5 V) and after the first discharge (1.5

V) processes which are denoted as A, B and C. As shown in Figure 7, the well ordered KS-6 gives very sharp peak at 26.5° indicating high crystalinity of KS-6. When the cell is charged to 3.5 V, the (002) peak shifts to 24.3° due to anion intercalation into the interlayer space of graphite. In addition another satellite peak appeared in the XRD at 33.1°. The intensities of these peaks are weaker than that of pristine peak. The new peaks provide profound evidence of the formation of a cation-graphite intercalation compound during the charging process. These observations are also in good agreement with previous literature [22-25]. During discharge, the peak position of the 002 peak did not completely regain to its original position. Instead, a broader peak appeared centering at 25.7° in the XRD pattern. This indicates a partial structural change of graphite during the initial charging process which cannot be fully recovered at the lower cut-off voltage in the cell. These partial structural changes may enhance the cycleability of the cathode. This is consistent with our previous observations, that during the discharge of full cell back to 0.0 V, the capacity retention is poor in the full cell.

Figure 7 shows the *ex-situ* XRD patterns of TiO_2 anode in its pristine state after first charge to 3.5 V and after first discharge to 1.5 V. The TiO_2 used in this study has an orthorhombic structure with a lattice parameters of a = 6.05 Å, b = 29.04 Å, and c = 3.86 Å. The charging of the full cell up to 3.5 V does not show significant changes in the XRD. At this stage the voltage of anode reaches 1.71 V vs. Li/Li^+. As shown in figure 7, when we consider the half cell of TiO_2/Li, the first discharge capacity of the TiO_2 anode is 208 $mAh.g^{-1}$. However, when it reaches to 1.71 V the discharge capacity is 105 $mAh.g^{-1}$, which is about 50 % of its full discharge. Therefore during the charging process of the full cell, the initial peak positions of TiO_2 do not show significant change. This could be attributed to the minimum structural changes of TiO_2 in this cell. Therefore no structural changes occur in the crystal lattice during the ceiling and bottom potentials of the cell. This was further confirmed by discharging the full cell back to 1.5 V.

The *ex-situ* XRD and electrochemical results could be used to elucidate the intercalation mechanism of $LiPF_6$ into graphite cathode and TiO_2 anode. Upon charging of the KS-6/TiO_2 full cell, Li^+ and PF_6^- ions in the electrolyte solution migrate towards their respective electrodes. The PF_6^- ions intercalate into the interlayer spaces of the graphite cathode electrode, while the Li^+ ions get into the TiO_2 anode. The first step of the charging process takes place in the voltage region from 0.0 to 2.6 V and involves adsorption of PF_6^- to the edge-plane surfaces of graphite which does not contribute appreciable capacity to the full cell. In the second step the charging reaction commences when potential exceeds 2.6 V and involves PF_6^- intercalation into KS-6 and Li^+ insertion into TiO_2. Therefore, this device is much safer than LIB in charged state. When the KS-6/TiO_2 cell is discharged, the Li^+ and PF_6^- ions are extracted from their respective electrode structures and reconstitute the original $LiPF_6$ electrolyte solution. These processes enable us to use the electrolyte as a sole source of Li^+ in this device.

4. CONCLUSIONS

A new energy storage system comprised of KS-6 cathode and TiO_2 anode is investigated in detail. The results suggest that the cathode to anode weight ratio and charging potential play dominant

roles and determine the cycle life of this device. KS-6/TiO_2 weight ratio 1 and operation voltage window 1.5-3.5 V were found to be optimum values allowing cycle life comparable to that of modern lithium ion batteries. The possibility to achieve long cycle life of graphitic cathodes undergoing deeper PF_6^- intercalation paves the way for development of electrochemical energy storage devices with transition metal free cathodes. These results demonstrate that the electrolyte could be used as the sole source of lithium ions. Charging voltage of KS-6 cathode could exceed 5 V vs. Li/Li+ without negative side effects such as oxygen release and excessive electrolyte decomposition. The suggested electrochemical device is inherently safer than lithium ion batteries and possesses higher energy density than conventional EDLC.

ACKNOWLEDGMENT
Partial financial support from Fukuoka Industry and Science Foundation is gratefully acknowledged.

References

1. D. H. Jurcakova, M. Seredych, Y. Jin, G. Q. Lu, T. J. Bandosz, *Carbon* 48 (2010) 1767.
2. P. Sharma, T.S. Bhatti, *A. Energy Conversion and Management* 51 (2010) 2901–2912
3. A. Bruke, *Electrochim.Acta* 53 (2007) 1083.
4. M. S. Whittingham, *Chem. Rev*. 104 (2004) 4271.
5. M. K. Song, S. Park, F. M. Alamgir, J. Cho, M. Liu, *Mater. Sci. Eng.* A, 72 (2011), 203.
6. W. Fergus, *J. Power Sources* 195 (2010) 939.
7. A. Du Pasquier, I. Plitz, J. Gural, F. Badway, G. G. Amutucci, *J. Power Sources* 136 (2004) 160.
8. A. Du Pasquier, I. Plitz, S. Menocal, G.G. Amatucci, *J. Power Sources* 115 (2003) 171–178.
9. A. Du Pasquier, I. Plitz, J. Gural, S. Menocal, G.G. Amatucci, *J. Power Sources* 113 (2003) 62–71.
10. 10. A. Du Pasquier, A. Laforgue, P. Simon, G.G. Amatucci, J.-F. Fauvarque, *J. Electrochem. Soc*. 149 (2002) A302–A306.
11. V. Khomenko, E. Raymundo-Pinero, F. Beguin, *J. Power Sources* 177 (2008) 643.
12. M. Yoshio, H. Nakamura, H. Wang, *Electrochem. Solid-states Lett*. 9 (2006) A561.
13. H. Wang, M. Yoshio, *Electrochem. Commun*. 8 (2006) 1481.
14. N. Gunawardhana, G.-J. Park, N. Dimov, A. K. Thapa, H. Nakamura, H. Wang, T. Ishihara, M.Yoshio, *J. Power Sources*, 196 (2011) 7886.
15. A. K. Thapa, G.-J. Park, H. Nakamura, T. Ishihara, N. Moriyama, T. Kawamura, H. Wang, M. Yoshio, *Electrochimica Acta* 55 (2010) 7305.
16. N. Gunawardhana, G.-J. Park, N. Dimov, A. K. Thapa, H. Nakamura, H. Wang, T. Ishihara, M.Yoshio, *J. Power Sources*, 203 (2012) 257.
17. H. Wang, M. Yoshio, *J. Power Sources*, 177 (2008) 681.
18. H. Wang, M. Yoshio, *Electrochem. Commmun*. 10 (2008) 382.
19. J.-W Lee, H.-l Kim, H.-J. Kim, S.-G. Park, *Appl. Chem. Eng*. 21 (2010) 265.
20. T. Brousse, R. Marchand , P.-L. Taberna, P. Simon, *J. Power Sources*, 158 (2006) 571.
21. M. Sasidharan, K. Nakashima, N. Gunawardhana, T. Yokoi, M. Inoue, S.-I. Yusa, M. Yoshio, T. Tatsumi, *Chem. Com*., 47 (2011) 6921.
22. J. A. Seel, J. R. Dhan, *J. Electrochem. Soc* 147 (2000) 892.
23. P. W. Ruch, M. Hahn, F. Rosciano, M. Holzapfel, H. Kaiser, W. Scheifele, B. Schmitt, P. Novak, R. Kotz, A. Wokaun, *Electrochim. Acta* 53 (2007) 1074.
24. T. Ishihara, Y. Yokoyama, F. Kozono, H. Hayashi, *J. Power Sources* 196 (2011) 6956.
25. G.-J. Park, N. Gunawardhana, C. Lee, S-M. Lee, M.Yoshio, *J. Power Sources*, 236 (2013) 145.